WCTE 2016
World Conference on Timber Engineering
August 22-25, 2016 | Vienna, Austria

LATERAL TESTING OF GLUED LAMINATED TIMBER TUDOR ARCH

Douglas R. Rammer[1], Philip Line[2]

ABSTRACT: Glued laminated timber Tudor arches have been in wide use in the United States since the 1930s, but detailed knowledge related to seismic design in modern U.S. building codes is lacking. FEMA P-695 (P-695) is a methodology to determine seismic performance factors for a seismic force resisting system. A limited P-695 study for glued laminated timber arch structures highlighted the lack of lateral load testing; therefore, critical modelling information was not available and assumptions based on available research were used. In this study, full-scale lateral load testing of the glued laminated timber arch is used to fill in gaps in test-based information and assess the following characteristics: damping, deformation behaviour, and failure modes.

KEY WORDS: Glued Laminated Timber, Arches, Seismic Design, Experiential, Failure

1 INTRODUCTION

Glued laminated timber arch structures are used with regularity in churches and other public buildings and assembly areas; however, ASCE/SEI 7-05 *Minimum Design Loads for Buildings and Other Structures* [1] does not provide guidance regarding the seismic design of these systems. Interim recommendations for seismic design of these systems provide seismic design coefficients for two classes of three-hinge arch systems: a special glued laminated arch and a glued laminated arch not specifically detailed for seismic resistance with use limited to seismic design category C and lower [2]. For special glued Laminated arch systems, required detailing provides additional strength in wood strength limit states and enables limited inelastic behaviour in connections through either wood bearing or fastener yielding.

A limited FEMA P-695 study of the glued laminated arch system was previously conducted and concluded with questions related to damping behaviour and strength limit states [3]. To address these questions, lateral load testing of a glued laminated arch was conducted. This paper presents frequency. damping, load-deflection behaviour, and failure limit states of three tested arches.

2 BACKGROUND

2.1 Arch Research

Research related to the performance of glued laminated arches started in the mid-1930s in the United States.

2.1.1 Vertical Loading Arches

In the 1930s, a considerable amount of research focused on development of glued laminated wooden members. One aspect was the, development of arches from thin, individual laminations of wood that could be bent into flowlag shapes. The highlight of the work was the construction and testing of a glued laminated arch building on the Forest Products Laboratory (FPL) campus [4]. The central arch line was loaded 30% above design criteria with sandbags for more than a year, and vertical deformations were recorded In addition, two arches were tested with thrust loading (Figure 1) and exhibited bending type failures in region between the arm and knee. In 2010, the glued laminated arch building was removed from service. The removed arches were loaded with a vertical loading that was representative of the sandbag loading to determine integrity of the arches after 75 years of service loading [5]. All arches except one showed no loss of structural performance to a loading that was 30% over the original design. One arch was deteriorated at the base. The presence of decay and delamination was attributed to the location of a steam vent in the building [6]. The only additional problem with the arches was the condition of peak connections. Due to insufficient end spacing, the wood at connection interfaces, developed wood shear plug failures. These local failures had little influence on global behaviour because the connection behaviour is mainly developed by wood bearing. Performance of glued laminated arches subjected to lateral loading has not previously been a focus of U.S. research.

[1] Douglas Rammer, USDA Forest Service, Forest Products Laboratory, USA, drammer@fs.fed.us

[2] Philip Line, American Wood Council, USA, PLine@awc.org

Figure 1: *Arch in testing frame*

2.1.2 Laterally Loaded Arches

Yasumura and Suziki [7] evaluated four glued laminated arch frames loaded with both a constant vertical load and a reverse cyclic lateral load. Three of the glued laminated arch frames contained an additional connection between the arch knee and arch peak. Only one of the framed arch specimens was a continuous wood member from base to peak and without additional mechanical joints between the arch knee and peak. Figure 2 shows the arch geometry used by Yasumura and Suziki [7] with no connections between the knee and peak along with positions of loads. A constant vertical load of 22.5 kN was applied while the increasing cyclic loading was applied until failure.

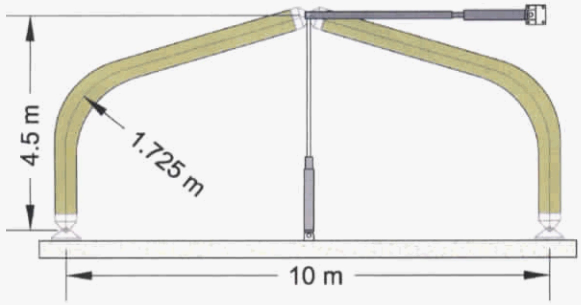

Figure 2: *Arch Specimen and Test Apparatus by Yasamura and Suziki*

Yasumura and Suziki noted that three arch frames, including the frame shown in Figure 2, failed in the curved part of the arch at low values of radial stress. An equivalent viscous damping value was obtained from the ratio of the absorbed energy to external work for each hysteric loop. For the arch containing no additional connection, the equivalent viscous damping was 1% to 2%, whereas the frames with connections had equivalent viscous damping of 2% to 3%. The development of radial failure increased viscous damping.

Building on Yasumara's work, Isoda [8] conducted a similar experimental study on several glued laminated timber arches with a newer appoach to connection design and no vertical loading. The observed arch failures emanated from the connection or occurred in the curved portion of the arch due to radial stress. He concluded that for this type of arch the equivalent viscous damping ratio was 6%. Although the findings of these two research programs are informative, the information generated was not used in the Charney and others [3] study because of the unique connections and low arch slopes.

2.13 Seismic Analysis of Tudor Arches

Although limited in scope, the study by Charney and others [3] implemented the FEMA P-695 methodology to evaluate the seismic response modification factor, R, for three-hinged glued laminated timber arches. FEMA P-695 [9] methodology was developed to give a rational approach for assignment of seismic design coefficients for the equivalent lateral force design procedure. The methodology is an iterative process that consists of nonlinear static and dynamic analyses on a number of prototypical building archetypes designed using the equivalent lateral force approach. The procedure also takes into account uncertainties inherent in test data and modelling methods. Charney and others [3] developed the building archetypes and conducted the incremental dynamic analysis using finite element procedures.

The study recommended steps that could both improve and validate the nonlinear time history analysis. Recommendations from the study were as follows:

1) Laboratory testing and improved nonlinear modelling of the base connection is recommended information obtained from such studies would allow for more realistic modelling of the stiffness and strength of base connections and could allow a revaluation for the P-695 uncertainty parameter that is associated with quality of test data

2) A realistic expression for period of vibration of glulam arch structures is needed. Development of such an expression could be obtained by analytical means alone hut, if possible, should be correlated with test results of full-scale specimens.

3) Dynamic full-scale tests on a three-hinge glued laminated arch system are recommended as a method of validating a damping assumption other than 2.5% critical assumed. Full-scale arch testing may also allow verification of structural models including connection models, particularly where nonlinear behaviour is considered.

2.2 Damping in Wood Structures

Damping dissipate stored energy and has the effect of reducing or restricting oscillations. Damping in structures is attributed to the materials of construction and connections within the structural system. Several studies have investigated the damping ratio for wood structures [7, 8, 10, 11, 12, 13]. For light wood-frame systems, the value range of equivalent viscous damping is 5% to 20%. For timber frame systems, such as wooden arches, values of equivalent viscous damping range from approximately 2% to 10%, depending on the types of connections and arch design.

3 EXPERIMENT PROCEDURES

3.1 SPECIMEN ARCH

The arched frames spanned 9.1m from outside face to outside face. The distance between arch frames for the prototypical archetype building was 3.66 m. A roof *gravity load of 718 N/m^2 and a wall gravity load of* 526N/m^2 were assumed between the arches.

To be consistent with design and construction practices in seismically active regions of the United States, technical representatives of the American Institute of Timber Construction were contacted to review the arch design and connection designs. Figure 3 and Table I describe the general details of the arch building as configured based on their input.

Glued laminated timber used in arch construction was Southern Pine, Combination 50 (1:10 slop of grain) produced in accordance with AITC A190.1 [14]. Uniform laminations were specified to facilitate use of smaller arch member size for the applied loads.

The base connection consists of a metal shoe and a 16-mm-diameter through bolt. The 16-mm-thick back plate was welded to the 13-mm side plates to provide bearing for outward thrust, and the bolt size and location are designed to transfer inward acting shear forces. The peak connection was a single 102-mm shear plate and 19-mm-diameter bolt designed to transfer shear forces (Figure 4). The arch member, bolted connection, and shear plate connection were designed in accordance with the *National Design Specification (NDS®) for Wood Construction.*

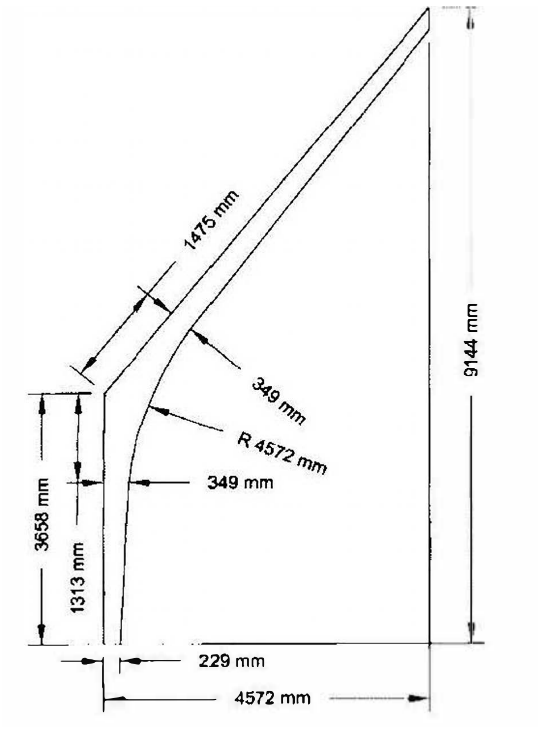

Figure 3: *Arch configuration*

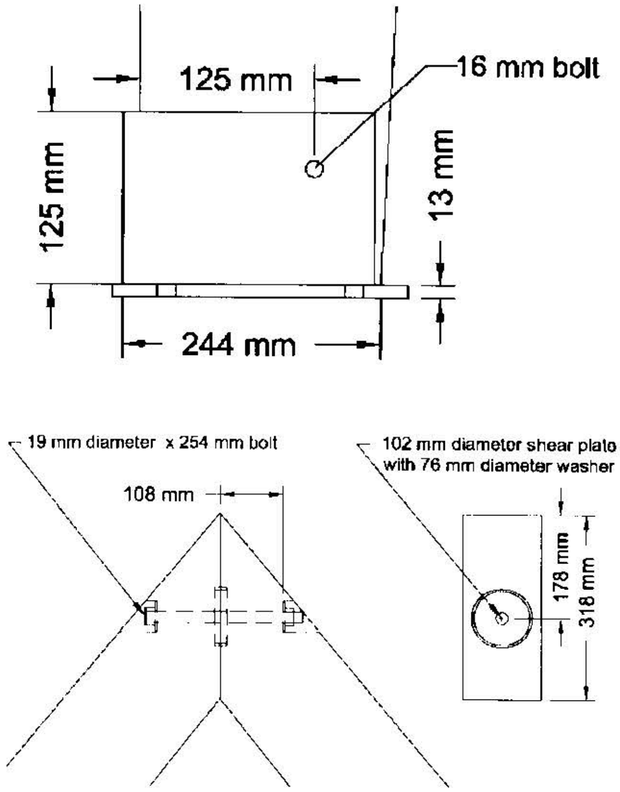

Figure 4: *Arch base and peak connection design*

Table 1 *Glued Laminated Arch Design Values*

Reference design value description	Design Values (MPa)
Bending	14.5
Modulus of elasticity	13,100
Shear design for loads causing bending about the *x-x* axis	1.5
Parallel to grain compression	13.8
Parallel to grain tension	9.3
Compression perpendicular to grain	5.1
Radial compression	5.1
Radial tension	0.5

3.2 MONOTONIC LOADING

Repeated cycles of vertical and lateral loads were applied to the arch frame. In all cases, the full vertical load was applied first and maintained constant while the lateral loading was varied. Lateral loading was applied in various steps as a percentage of the reference lateral load. Lateral loading steps were 10%, 25%, 50%, 100%, and 150% of reference load level. This was followed by a monotonic load to failure. The rate of loading was constant. Figure 5 shows the entire loading protocol as a function of time. After the 50%, 100%, and 150% steps, the lateral and vertical actuators were detached from the arches to evaluate damping.

The upper slope of the glued laminated arch made it difficult to secure a uniformly distributed load to the upper arch structure. Instead, the vertical gravity design load was applied using two actuators attached to the strong floor that were free to rotate and displace to maintain a constant gravity load of 12.0 kN on each arch. The concentrated vertical load was placed to maintain similar base connection reactions in the distributed and concentrated loading cases. Vertical actuators were attached to the upper surface of the arch and to the floor at a distance of 1346 mm from the outside face of each arch.

For application of lateral load, two MTS 406+mm actuators pushed and pulled the arch at a height of 3850-mm above the base of the arch. Because the deformation of the west and east knee are not the same, both actuators were loaded under force control until final loading to failure. For Arch 1, final loading to failure used displacement control as a safely precaution. For Arch 2 and 3 tests, final loading to failure used actuators in force control.

To maintain the arch in a vertical plane during loading, a steel frame was constructed (Figure 6). Teflon pads were placed between the steel frame and the arch to allow for free movement while maintaining the arch in the vertical plane.

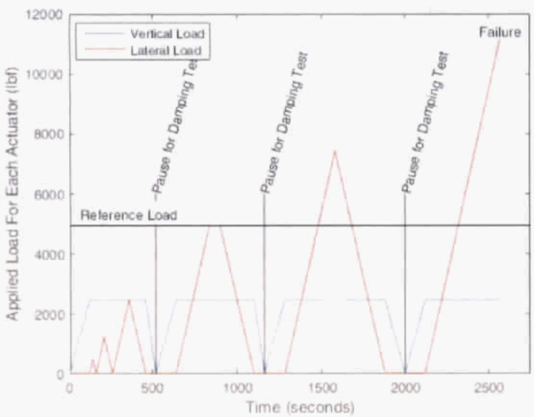

Figure 5: *Monotonic loading protocol*

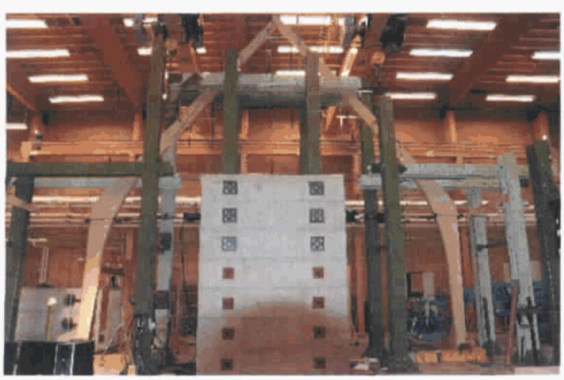

Figure 6: *Arch frame within the steel support frame*

3.3 DAMPING TESTS

Prior to any applied load and after the 50% 100%, and 150% of the reference lateral loads were applied, a series of nondestructive damping tests were conducted. A small rotatory motor with an eccentric mass was located approximately 3500 mm from the floor on the east arch. The frequency of the motor was adjusted from approximately 2.8 to 4.2 Hz, and lateral displacements of both the east and west knees were recorded.

3.4 MEASUREMENTS

Deformations were recorded using traditional string potentiometers or LVDTs and with calibrated cameras tracking targets on the arch for the quasi-static loading (Figure 7). Measurements were recorded at 1 sample per second until the ramp load to failure, where the sample rate was increased to 10 samples per second.

For damping tests, lateral displacements of both the cast and west knees were sampled at rate of 200 samples per second.

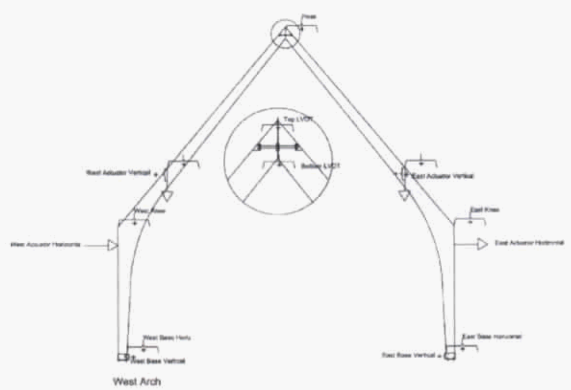

Figure 7: *Measurement and concentrated load locations*

4 EXPERIMENTAL RESULTS

4.1 DAMPING TESTS

Damping tests were conducted at four levels for each of the arches tested. Because the time the motor was maintained at each frequency was inconsistent, the data were analysed by calculating the frequency and amplitude for successive 1200-point windows for all points. Normalized displacement amplitude was plotted as a function of frequency (Figure 8). To determine the equivalent viscous damping ratio, a half-power method was used. In this approach, first the peak normalized amplitude response is located. Next a horizontal line is drawn across the response curve at a level equal $1/\sqrt{2}$ times the peak response. The frequency difference between where the horizontal line intersects the response curve divided by the natural frequency is twice the equivalent viscous damping ratio (i.e., the frequency difference divided by the natural frequency).

Table 2 lists peak frequency and calculated damping ratios for the tested arches. For the second arch, damping tests after 50% loading were not conducted. For the first arch, the peak frequency averaged 3.56 Hz until loaded to 150% of the reference load, while the equivalent viscous damping ratio was between 2.65% and 3.44%.

For the second arch, peak frequency was consistent and averaged 3.78 Hz, while the damping ratio was changed with increasing loading cycles. For the first loading, the equivalent viscous damping ratio was 3.17%, but after the loading at 50% of reference load the remaining damping measurements were above 5%.

For the final arch, peak frequency and equivalent viscous damping ratio were consistent and averaged 3.49 Hz and 2.16%, respectively.

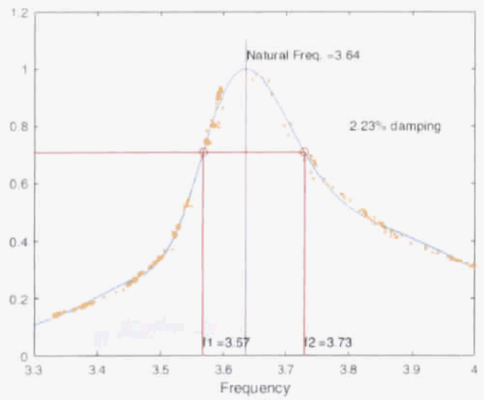

Figure 8: *Analysis of natural frequency and damping*

Table 2 *Frequency and Damping Results for Arches*

Specimen	Reference Load Level (%)	Peak Response Frequency (Hz)	Damping Ratio (%)
Arch 1	0	3.60	3.30
	0	3.59	3.44
	50	3.54	2.65
	100	3.51	3.07
	150	3.82	3.24
Arch 2	0	3.81	3.17
	0	3.79	2.34
	100	3.79	5.03
	150	3.76	5.25
Arch 3	0	3.55	2.09
	50	3.45	2.25
	100	3.46	2.14

4.2 MONOTONIC LOADINGS

4.2.1 Arch 1

Arch 1 failed in the curve portion due to radial stress and a split emanating from the peak connection in the west arch (Figure 9). A detailed review of the video showed that the radial failure occurred first. For the final loading to failure of Arch 1, the lateral load actuators were driven in displacement control due to safety concerns. The actuator contro1 profile was generated using displacements recorded in the loading to 150% design level. For actuator displacements beyond the 150% design load level, the displacement rate of each actuator was set based on the previous 30 s of loading. Unfortunately this loading approach led to the west actuator applying a load 10% greater than the east actuator at the time of failure. The implications of this will be discussed later in the paper. At failure, the total applied load to the arch was 77.0kN, 40.7kN for the west actuator and 36.4kN for the east actuator. Load versus horizontal displacement of the west knee was linear to failure, whereas the load versus east knee displacement was nearly linear until the last inch of applied deformation.

Figure 9: *Radial tension failure for first tested arch*

4.2.2 Arch 2

Arch 2 failed in the west arch due to flexural bending in the region between the peak connection and knee (Figure 10). Based on experience from testing Arch 1, Arch 2 was loaded in force control to maintain the lateral force requirements to failure. The total laterally applied force was 82.8kN, 41.4kN for the west actuator and 41.4kN for the east actuator. The plot of each actuator load versus horizontal displacement of the corresponding knee was nearly linear until to failure. Only slight nonlinear deformation was observed near failure. During the 150% of design loading, the haunch section of the east arch began delaminating. To arrest the delamination in the final test to failure, 102-mm self-tapping screws were inserted from the top side of the arch.

4.2.3 Arch 3

Arch 3 failed below the 150% reference load level in the west arch at a finger joint located approximately 3.85 m above the base and within the radius of the knee (Figure 11). Figure 11 also shows that the failure crack progressed along the arm toward the arch peak. Arch 3 was loaded in force control to maintain the lateral force requirements to failure. The total laterally applied force was 60.9kN, 30.5 kN for the west actuator and 30.4kN for the east actuator. The plot of each actuator load versus the horizontal displacement of the corresponding knee was nearly linear until to failure. During the 100% of reference loading, the east haunch section began delaminating and 102-mm self-tapping screws were inserted from the top side of the arch to arrest the crack formation.

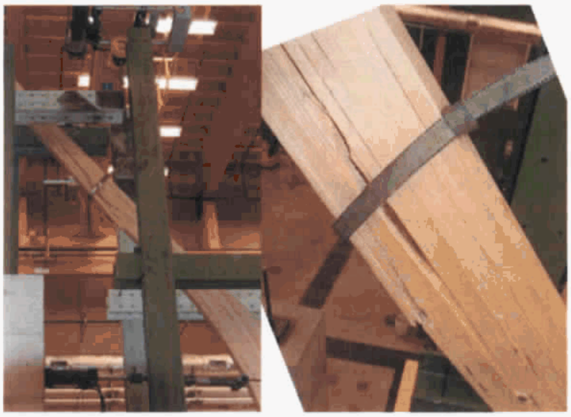

Figure 10: Bending failure of west arch during second test

Figure 11: Failure of west arch at finger joint during third test

4.3 Connection Observations

4.3.1 Base Connections

Although the global behaviour of the arch frame seems linear to failure, significant nonlinear behaviour was observed in the base connections. Figure 12 shows the surface wood crushing and the deformed bolts after failure loading for the west base. This base resists the inward shear and uplift forces from lateral loading. The resulting bolt deformation and wood crushing are consistent with NDS Yield Mode IIIs design condition. Furthermore, the permanent deformation and level of wood crushing indicates the connection experienced inelastic behaviour.

Figure 13 shows the surface wood crushing and the deformed bolts after failure loading for the east base. While perpendicular to grain bearing on the shoe is the design limit state condition, the resulting wood crushing and bolt deformation indicate the fastener is assisting to limit the rotation of the arch leg. The resulting bolt deformation and pattern of wood crushing indicates nonlinear behaviour consistent with NDS Yield Mode IIIs design condition.

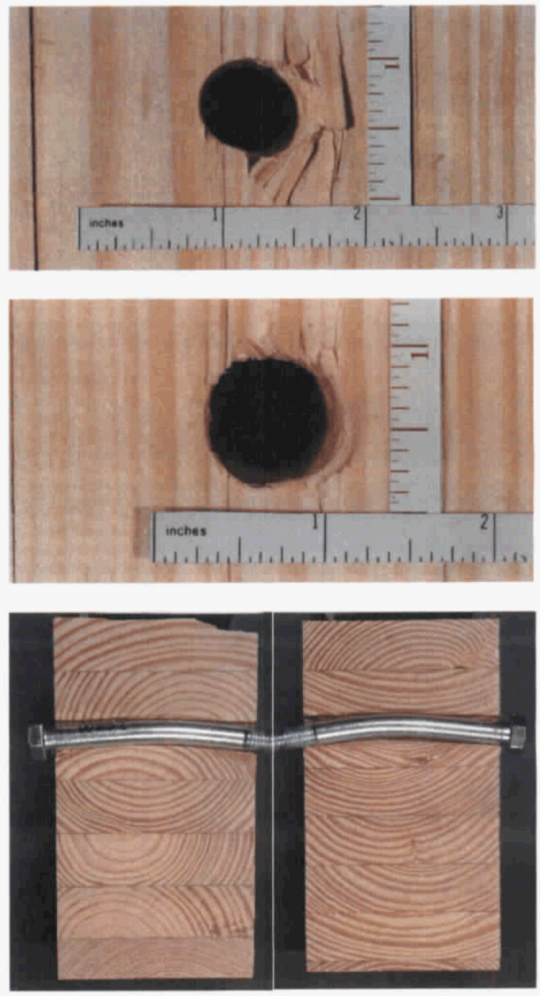

***Figure 12:** West base connection deformations.*

4.3.2 Peak Connection

Figure 14 shows the peak connections after the arches were loaded to failure. The left image of the shear plate connection from west side Arch 1 shows splitting wood emanating from the upper half of the shear plate. These splits were present for 260 mm down the arm. The right image of the shear plate connection for the west side of Arch 2 shows no wood failure. In contrast, the top bolt for Arch 1 shows no permanent deformation, whereas the top bolt from Arch 2 shows permanent deformation. Although not visible in the images, the wood surfaces below the shear plate had evidence of surface contact and crushing.

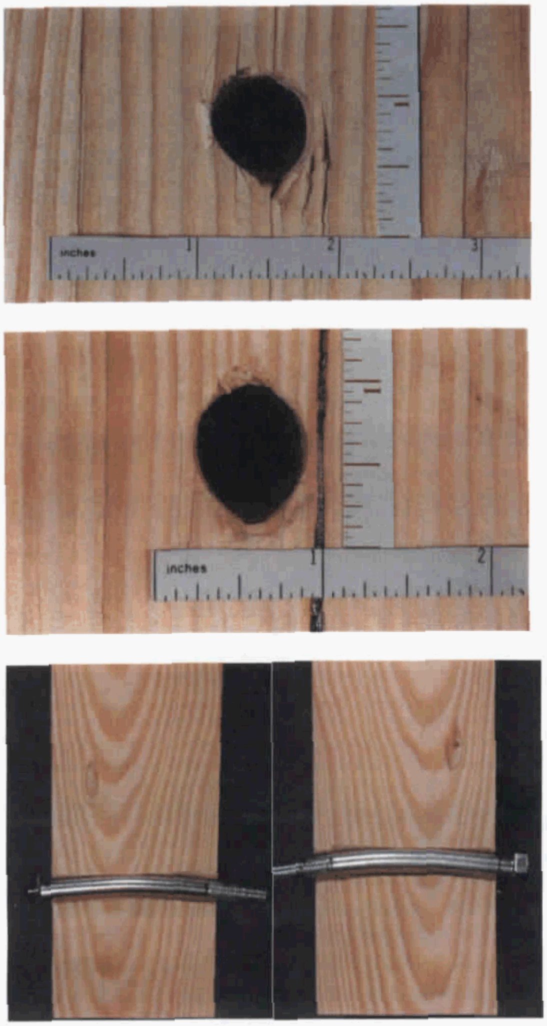

Figure 13: *East base connection deformations*

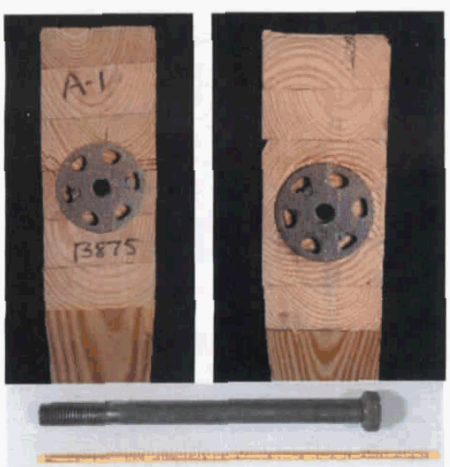

Figure 14: *Peak connection post failure*

4.4 LoadFactors

Total lateral load at failure, total lateral load for design stress ratio equal to 1.0, and the resulting load factors are summarized in Table 3. For all arches, the controlling design limit state producing design stress ratio equal to 1.0 was due to bending in the west arch arm. For purposes of calculating the design stress ratio, lateral loading was assumed to be equally distributed between west arch and east arch and acting in combination with gravity load. Although Arch 3 had the smallest value of lateral load for stress ratio equal to 1, it exceeded the factor used (i.e., approximate 1.82 factor) in the analytical study by Charney and Others [3] and for all three tested arches, the average load factor, or the ratio of load at failure to the lateral load for stress ratio equal to 1.0 for all tests, is equal to 2.35.

Table 3 *Load Factor for Arches*

Specimen	Total lateral load at failure (peak load) (kN)	Total lateral load for 1.0 design stress ratio (kN)	Load factor
Arch 1	77.0	31.1	2.5
Arch 2	82.2	31.1	2.6
Arch 3	60.9	31.1	2.0

4.5 Horizontal Displacement at Peak Load

As noted previously, horizontal displacements at arch knees were nearly linear to failure. Horizontal displacement of the west knee and east knee for each arch is summarized in Table 4.

Table 4 *Horizontal Displacement at Peak Load for Arches*

Specimen	West knee (mm)	East knee (mm)
Arch 1	206	186
Arch 2	216	203
Arch 3	176	175

5 ANALYTICAL MODELLING

The radial tension failure to Arch 1 led to analytical modelling of the arch frame to investigate radial stresses within the knee region and implications of the west actuator load being 10% higher than the east actuator at failure.

A 2D finite element model was developed with ADINA [16] using nine node quadrilateral elements with linear elastic orthotropic material properties for the glued laminated arches. Contact elements were incorporated into the model to capture the uplift and nonuniform contact of the arch bases in the shoes and the surface bearing contact occurring at the peak connection. The translation was fixed at the base bolt location. Figure 15 shows a representative mesh of the arch model. Loads were applied uniformly over the contact area. Vertical loads were applied and maintained in the vertical direction, whereas the experimental gravity load changes direction as the lateral loads were applied. Because angle changes in the experiments were small, it is assumed the effect was negligible.

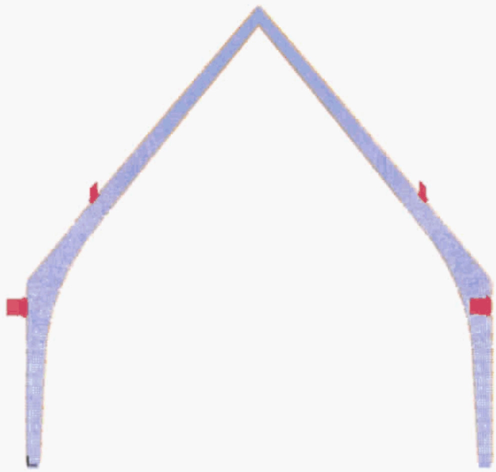

Figure 15: ADINA analysis model

The arch FE model was validated by comparing the analytical and experimental deformation at the design load (Figure 16). Good agreement was observed once the contact elements were included in the preliminary models.

Applying measured loads at failure for the unequal actuator distribution on Arch 1 resulted in the radial stress profile shown in Figure 17 for the west knee. Figure 18 shows the radial stress distributions for the case where total load at failure is equally distributed to each arch.

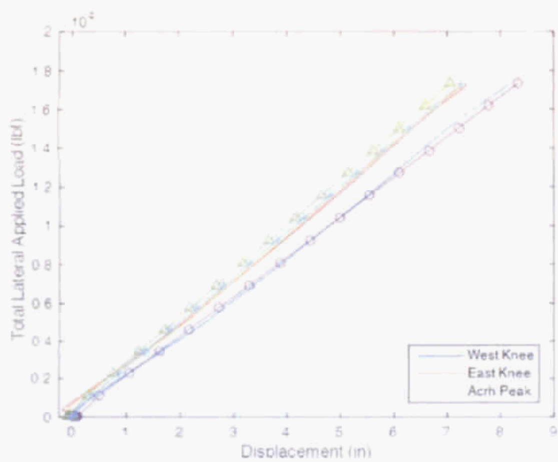

Figure 16: Comparison of model and experimental knee and peak deformation for 150% design loading

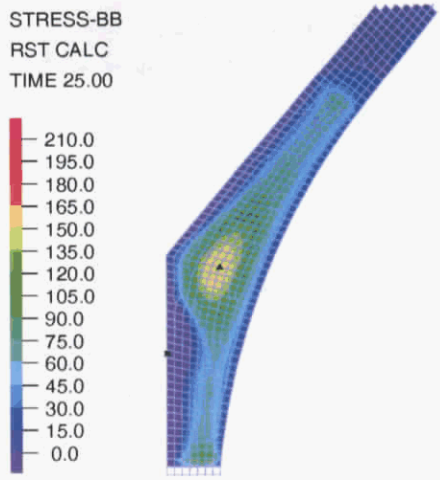

Figure 17: Radial stress distribution in the west arch for unequal actuator loading

Comparison of the stress profiles shows a similar stress distribution, but the unequal actuator distribution had slightly higher radial stress. Although there is a difference, the difference Is small. The maximum radial stress for the unequal actuator loading is 1.076 MPa, whereas the maximum radial stress for the equal actuator loading is 1.034 MPa, a difference of less than 5%. Therefore it is concluded that the effect of unequal loading was insignificant.

Arch2 failed in bending at 1500 mm from the outside face of the arch. Figure 16 shows the longitudinal stress distribution for the arch between the knee and peak at failure from the FE analysis. A maximum tensile stress of 39.7 MPa is shown by the triangle in the distribution. Both the predicted and actual failure locations are similar. A ratio of tensile stress at failure, as determined by FE analysis, to allowable design tension stress is 1.71. Similarly, the maximum radial tensile stress in the knee as determined by FE analysis was 1.103 MPa, above the Arch 1 values. The ratio of radial tension stress at failure to design radial tension stress was approximately 2.2.

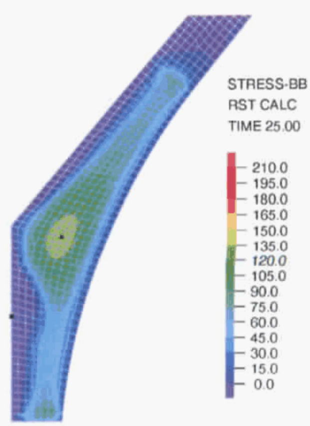

Figure 18: Radial stress distribution in the west arch for evenly distributed actuator loading

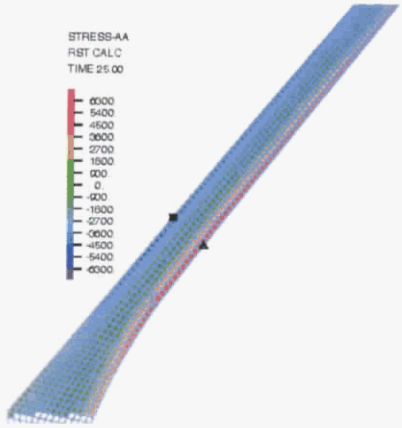

Figure 19: *Longitudinal stress distribution in the west arch arm for Arch 2 at failure.*

6 CONCLUSIONS

Three glued laminated timber arch frames were tested to better understand damping, load-deformation behaviour, and failure limit states of this system. Arch 1 peak frequency averaged 3.56 Hz until loaded to 150% of the reference load, while the damping ratio was between 2.65% and 3.44%. A radial tension failure in the west arch was the observed failure mode.

Arch 2 peak frequency was consistent and averaged 3.78 Hz, while the equivalent viscous damping ratio was changed with increasing loading cycle. For the first loading, the critical damping was 3.17%, but after the loading of 50% of referance, the remaining equivalent viscous damping ratio measurements were above 5%. A flexural failure of the west arch between the knee and peak was the observed failure mode.

Arch 3 peak frequency averaged 3.49 Hz for loading up to 100% of the reference load, while the equivalent viscous damping ratio was nearly constant at 2.16%. Failure occurred at a finger joint locate in the knee section of the arch. It is noted, that all three failures were located in the west arch with was experiencing uplift forces.

The global arch load-deformation response was essentially linear-elastic to failure; however, significant nonlinear behaviour was observed in the base connections. The bolts were permanently deformed and the wood was crushed throughout the cross section.

ACKNOWLEDGEMENT

The authors acknowledge Sentinel Structures for the fabrication of the glued laminated arches and design assistance from the AITC member engineers.

REFERENCES

[1] ASCE 7: Minimum Design Load for Buildings and Other Structures, American Society of Civil Engineering, Reston, VA 2005.

[2] FEMA P-750: NEHRP Recommended Seismic Provisions for New Buildings and Other Structures, Part 3 Resource Papers, Federal Emergency Management Agency, Washington, D.C., 2009.

[3] Charney F., Eberle J., Line, P., Kochkin V.: Seismic Analysis of Three-hinge Glulam Tudor Arches Using the P695 Methodology. Proceedings of the 2014 World Conference on Timber Engineering. Quebec, CA. 2014.

[4] Wilson T.R.C.: The Glued Laminated Wooden Arch. USDA Technical Bulletin No. 691, 1939.

[5] Rammer D.R., Moura J.: Structural Evaluation of the Second Oldest Glued-Laminated Structure in the United States. USDA Forest Service, Forest Products Laboratory, General Technical Report, FPL-GTR-226. pp. 269-276, 2013

[6] Teder M., Wang X.: Nondestructive Evaluation of a 75-Year Old Glulam Arch. USDA Forest Service, Forest Products Laboratory, General Technical Report, FPL-GTR-226, pp. 624-632, 2013.

[7] Yasumura M., Suzuki.: Lateral Loading test on Glued-laminated Arched Frames, Summaries of technical Papers of Annual Meeting Architectural Institute of Japan, 1992.

[8] Isoda H.: Pseudo---Dynamic Test and Evaluation of The Maximum Response of a Glulam Frame Under Big earthquake Attack. World Congress on earthquake Engineering, 2000.

[9] FEMA (2009). FEMA P-695: Quantification of Building Seismic Performance Factors, Federal Emergency Management Agency, Washington, D.C.

[10] Yeh, C.T., Hartz, B.J., Brown, C.B: Damping Sources in Wood Structures. Journal of Sound and Vibration, Vol 19(4):411-419, 1971.

[11] Polensek. A.: Damping capacity of nailed wood joist floors. Wood Sci. 8(2):141. 1975.

[12] Polensek, A.: Damping of roof diaphragm with tongue and groove decking. Wood Sci. 9(2):70. 1976

[13] Sutoyo, D., Hall, J.. Study of Wood-Frame Building Records From Parkfield and San Simeon Earthquakes. SMIP06 Seminar Proceedings, 2006.

[14] ANSI 190.1 Standard for Wood Products - Structural Glued Laminated Timber. APA- The Engineered Wood Association, Tacoma, WA. 2012.

[15] Clough R, Penzien: Dynamics of Structured, 3rd Edition McGraw-Hill Companies. 634p, 1985.

[16] ADINA System 9.2.2. ADINA R & D, Inc., Watertown, MA USA 2016.